JSHC
Japan Society of Histochemistry and Cytochemistry
Established 1959

Acta Histochem. Cytochem. 56 (5): 77–86, 2023
doi: 10.1267/ahc.23-00027

Regular Article

Beneficial Effect of Erythropoietin on Ameliorating Propionic Acid-Induced Autistic-Like Features in Young Rats

Sara A. Hosny[1], Alshaymaa M. Abdelmenem[2], Taha Azouz[3], Samaa S. Kamar[1], Asmaa M. ShamsEldeen[4] and Asmaa A. El-Shafei[1]

[1]Histology Department, Faculty of Medicine, Cairo University, Manial, Cairo, Egypt, [2]Histology Department, Faculty of Medicine, Fayoum University, Egypt, [3]Medical Biochemistry Department, Faculty of Medicine, Cairo University, Manial, Cairo, Egypt and [4]Physiology Department, Faculty of Medicine, Cairo University, Manial, Cairo, Egypt

Received May 1, 2023; accepted August 22, 2023; published online October 4, 2023

Autism is a neurodevelopmental disorder that impairs communication and social interaction. This study investigated the possible beneficial effects of erythropoietin (EPO) on experimental autistic-like behaviors induced by propionic acid (PPA). Twenty-four rats were distributed into three groups: (i) control; (ii) PPA_Gp: daily injected subcutaneously with PPA for five consecutive days; PPA+EPO-Gp: injected with PPA, then received intraperitoneal injection of EPO once daily for two weeks. Behavioral changes in the rats were assessed. Specimens from the cerebellar hemispheres were subjected to histological and ultrastructure examination, immunohistochemistry for glial fibrillary acidic protein (GFAP) and calbindin-D28K, and biochemical analysis for glutathione peroxidase (GSH-Px), malondialdehyde (MDA), gamma amino-butyric acid (GABA), and serotonin. PPA-Gp showed significant behavioral impairment, with a significant depletion in GSH-px, GABA, and serotonin and a significant increase in MDA. Histological examination revealed reduced Purkinje cell count with ultrastructural degeneration, irregularly arranged nerve fibers in the molecular layer, astrogliosis, and significantly decreased calbindin-immunostaining compared to the control. EPO protected cerebellar structure, increased Purkinje cell count, improved neuronal morphology, reduced PPA-induced autistic-like features, alleviated neuronal oxidative stress, increased intercellular antioxidant levels, and suppressed inflammation. EPO provided significant protection against PPA-induced autistic features in rats, with structural preservation of Purkinje cells.

Key words: Purkinje cells, autism, calbindin D28K, GFAP, GABA

I. Introduction

Autism spectrum disorder (ASD) is a neurodevelopmental disorder characterized by impaired communication and social skills, repeated and disorganized movements, sensory abnormalities, and occasional self-injury. Recently, there has been considerable evidence that the cerebellum is a major organ affected in ASD and plays a paramount role in autism pathophysiology [36]. Postmortem pathological examination of autistic brains demonstrated decreases in the gray and white matter of the cerebellum, with decreased size and number of Purkinje cells (PC) and output neurons in the cerebellum [17].

The short-chain fatty acid PPA is synthesized by gut microorganisms as a fermentation product and is a commonly used food preservative. Massive intake of processed foods with high amounts of PPA is a leading cause of autism, particularly in pregnant women, with an increased risk in newborns [1]. It passes through the gut-blood and blood-brain barriers and is taken up by neuronal cells, causing intracellular acidification, which affects neurotransmitter release and causes neuroinflammation, enhanced

Correspondence to: Samaa Samir Kamar, Histology Department, Faculty of Medicine, Cairo University, Egypt, 11559.
E-mail: Samaakamar@cu.edu.eg

oxidative stress, and glutathione depletion [23]. These induce behavioral exacerbations and autism-like features [6].

Erythropoietin (EPO) is a glycoprotein hormone that plays a pivotal role in erythropoiesis. Within the central nervous system, EPO receptors (EPO R) are expressed in the cerebral cortex, midbrain, hippocampus, internal capsule [24], and cerebellar granule cells [19]. Moreover, EPO receptors are expressed in the brain capillaries and end-feet of astrocytes, suggesting that circulating EPO is transferred into the brain tissue [11]. Several studies have demonstrated the neuroprotective and neurotrophic efficacy of EPO in various neuropsychiatric disorders, including neurodegeneration [26], epilepsy [34], Alzheimer's disease [29], and traumatic brain injury [9]. In animal studies, EPO showed a modulatory effect on neurogenesis as well as anti-inflammatory, antioxidant, and anti-excitotoxic properties [37]. It is also linked to improved memory and learning performance [33].

This study assessed the possible neuroprotective effects of EPO in a PPA-induced autism model in young male rats using histological, immunohistochemical, electron microscopy, and biochemical studies correlated with morphometric and statistical analyses.

II. Materials and Methods

Drugs

Propionic acid was used as a solution of ≥ 99.5% (500 mL) (Sigma-Aldrich, St. Louis, Missouri, U.S.). Erythropoietin; "EPREX®" in the form of 0.4 ml prefilled syringes containing 4000 I.U. of recombinant human erythropoietin (r-HuEPO) (Santa Farma, Istanbul, Turkey).

Animals

Twenty-four young Wistar male albino rats, at 3 weeks of age and weighing approximately 100 g, were housed in ventilated cages at 24°C in Kasr Al Ainy Animal House, Cairo University, and fed ad libitum throughout the experiment. The experimental protocol was approved by the Institutional Animal Care and Use Committee (IACUC) of Cairo University (approval no. CU-III-F-48-22).

Experimental design

Wistar rats [35] were equally distributed into three groups (n = 8), with four rats per cage, as follows: (i) control rats; (ii) PPA-Gp: each rat received 500 mg/kg (250 mg/mL, pH 7.4) of PPA by subcutaneous injection once daily for five consecutive days, then left for two weeks [6]; (iii) PPA+EPO-Gp: each rat received PPA as in PPA-Gp for five consecutive days, followed by intraperitoneal injection (IPI) of EPO at a dose of 5,000 U/kg once daily for two weeks [21].

At the end of the experiment, all rats were subjected to neurological examination using the elevated plus-maze and social interaction tests to assess the progression of autistic features. The rats were then sacrificed by IPI of ketamine-xylazine (100 mg/kg), followed by transcardial perfusion with 10% formalin until the liver was cleared [15]. The cerebellum of each rat was dissected and divided into two hemispheres for biochemical and histological analysis.

Functional neurological examination

Behavioral assessment and procedures using the elevated plus maze test

All rats were examined neurologically to detect anxiety-like behavior. Each rat was allowed to explore the maze for 5 min in a four-armed elevated plus maze, and their behavior was recorded using a video camera. The recorded behaviors were the time spent in the free arms, the number of entries made in the open arm, the number of head dippings, and the duration of grooming. The elevated plus maze consisted of a central square and four arms: two arms without walls (open arms) and two arms enclosed by 40 cm high plastic walls (closed arms), and each arm was 50 × 10 cm in dimensions. The arms were elevated from the ground by 50 cm [13].

Behavioral assessment and procedures using social interaction tests

The day before the experiment, rats were housed separately. The following day, after 60 min of habituation in the experimental room, the examination was performed using a white apparatus (a 50 × 40 × 40 cm box) [39]. The test was performed by exposing each rat from one group to another unfamiliar rat (control versus control or PPA-Gp versus PPA-Gp) for 20 min [6]. The percentage (%) of engagement time was calculated. Mounting, grooming, and sniffing body parts were considered indicators of social interaction and engagement [14].

Biochemical study

Part of the right cerebellar hemisphere of each rat was thoroughly ground using a manual grinder in 0.05 M PBS (pH 7.4) as a 0.01% weight/volume of tissue homogenate buffer (0.7 mg tissue in 7 ml buffer). The supernatants were separated by centrifugation for 2 min at 2000 × g to separate the supernatants [2] at the Department of Medical Biochemistry, Faculty of Medicine, Cairo University, to assess the following parameters:

- Glutathione peroxidase: using tert-butyl hydroperoxide as a peroxide substrate
- Malondialdehyde: Thiobarbituric acid-reactive by-products of lipid peroxidation (TBARS)
- Gamma amino-butyric acid: ELISA immunoassay kit was supplied by ALPCO Diagnostics (Salem, NH, USA) and performed according to the kit's instructions.

The serotonin ELISA immunoassay kit was supplied by Immuno-Biological Laboratories (IBL, Hamburg, Germany) and was performed according to the manufacturer's instructions.

Quantitative real-time polymerase chain reaction (qRT-PCR) of EPO R

Quantitative expression of the EPO R gene was assessed using qRT-PCR. The homogenized cerebellar samples of all study groups were processed, total RNA was extracted using TRIzol (Life Technologies, USA), and single-stranded cDNA was produced using the Thermo Scientific cDNA kit (#K4374966) for RT-PCR. Equal amounts of cDNA were then used for the subsequent PCR, which was conducted using GoTaq Green Master Mix (Promega), PCR-grade water, and specific primers for EPO receptor (Forward Primer: 5'-TTCAGCGGATTCTGGAGTGCCT-3', Reverse Primer: 5'AGCAACAGCGAGATGAGGACCA-3'). The data were computed using the Sequence Detection Program version 1.7 (PE Biosystems, Foster City, CA, USA). The comparative Ct method (Applied Biosystems, USA) was used to determine the relative expression levels to β-actin (housekeeping gene), according to the manufacturer's instructions: forward primer β-actin, 5'-GGAGATTACT GCCCTGGCTCCTA-3'; β-actin reverse primer, 5'-GACTCATCGTACTCCTGCTTGCTG-3'.

Histological studies

The left cerebellar hemispheres were fixed in 10% formalin in 0.1 M phosphate-buffered saline for 48 hr and then processed into paraffin blocks. Serial sections of 5 μm thickness were subjected to the following:

(a) Hematoxylin and eosin (H&E) staining to illustrate morphological changes.
(b) Bielschowski's silver (Ag) method for neurofibril demonstration [4].
(c) Immunohistochemical staining was performed using the following formula:
    1- Anti-GFAP, a mouse monoclonal antibody (Lab Vision Corporation Laboratories, U.S., Cat. # MS-1376-P0, dilution 1:100) to identify astrocytes
    2- Anti-calbindin D28K antibody (D-4) and mouse monoclonal antibody (Santa Cruz Biotechnology, U.S., Cat. # sc-365360; dilution 1:100) to demonstrate PCs.

For immunohistochemical staining, sections were deparaffinized, rehydrated, and retrieved in 10 mM citrate buffer (pH 6) under heated conditions for 30 min, and then incubated overnight with the primary antibodies in a humidity chamber. Incubation with the mouse/rabbit polydetector DAB HRP Brown Detection System (Bio SB, China, Cat. # BSB 0201S) was performed for 45 min at room temperature in humidity chamber. Immunohistochemical staining was performed using diaminobenzidine as a chromogen and counterstained with Mayer's hematoxylin.

Electron microscopy

About 1 mm^3-sized specimens of the cerebellar cortex were first fixed in 2.5% glutaraldehyde (pH 7.4) and then post-fixed in 1% osmium tetroxide. To contrast the ultrathin sections (60–70 nm), they were mounted on copper grids and stained with uranyl acetate and lead citrate. A transmission electron microscopic (TEM) analysis was performed using a JEM-1400A TEM (JEOL, Tokyo, Japan) operated at 80 kV at the Faculty of Agriculture Research Center, Cairo University.

Morphometric study

Using Olympus light microscope (Japan) connected to a "Leica Qwin 500C" image analyzer system (Cambridge, UK) at the Histology Department, Faculty of Medicine, Cairo University, eight randomly chosen high-power fields (× 400)/section in each group were examined to obtain the following parameters:

(a) Purkinje cell count in H&E-stained sections
(b) Optical density of the Ag-positive reaction in the molecular layer of Ag-stained sections
(c) Area % of GFAP-immunopositive astrocytes
(d) Optical density of calbindin D28K immunopositive cells in immunostained sections

Statistical analysis

Statistical Package for Social Science software, version 16 was used to evaluate and compare biochemical and morphometric measures. One-way analysis of variance and post hoc Tukey tests were used to compare the different groups with the control group, and all data was presented as mean ± standard deviation (SD). Correlations between quantitative variables were determined using Pearson's correlation coefficients. Statistical significance was set at $p < 0.05$.

III. Results

Amelioration of anxiety and social deficits with EPO

As shown in (Table 1), the results obtained from the elevated plus maze included the number of open arm entries, time spent in the open arm, and number of head dips, all of which indicated risk assessments. These values were significantly lower in the PPA-Gp group than those in the control group. However, they showed improvement in PPA+EPO-Gp compared to PPA-Gp. The duration of grooming indicated that anxiety was significantly increased in PPA-Gp compared to the control group and significantly decreased in PPA+EPO-Gp compared to PPA-Gp. Social interaction was also assessed. The current results reported a significant decrease in the duration of social interaction in the PPA-Gp group compared to the control group, and an improvement was observed in PPA+EPO-Gp compared to PPA-Gp.

Change in the level of GSH-Px, GABA, serotonin, and MDA levels with EPO

The PPA-Gp showed a statistically significant decrease in the mean values of GSH-Px, GABA, and serotonin levels, which were associated with a significant increase in the mean values of MDA levels in comparison

Table 1. *The result obtained from elevated plus maze and social interaction test for all the experimental groups (n = 8)*

Neurological assessment	Control	PPA-Gp	PPA+EPO-Gp
No of open arm entry	5.25 ± 1.04	2.25 ± 1.04*	4.5 ± 1.2#
The time spent in open arm (sec)	30.13 ± 3.87	11.63 ± 2.67*	22.38 ± 2.97*#
Head dips	22.75 ± 3.11	8.25 ± 1.98*	18 ± 2.14*#
Duration of grooming (sec)	7 ± 1.69	21 ± 3.82*	11.38 ± 2.33*#
Interaction time (sec)	174.88 ± 5.28	59.12 ± 6.94*	97.12 ± 6.94*#

* Sig (≤ 0.05) versus the control Gp; # Versus PPA-Gp.

Table 2. *The mean values (± SD) of GSH-Px, MDA, GABA, serotonin and EPO R levels in the control and the experimental groups (n = 8)*

Groups	GSH-Px (mmol/mL)	MDA (nmol/mL)	GABA (ng/mg)	Serotonin (ng/mg)	EPO R
Control	6.19 ± 1.53	12.56 ± 1.29	93.38 ± 8.49	7.83 ± 1.29	1.01 ± 0.01
PPA-Gp	1.88 ± 1.28*	25.78 ± 2.21*	76.87 ± 7.02*	4.25 ± 0.96*	1.63 ± 0.06*
PPA+EPO-Gp	5.59 ± 1.84#	12.49 ± 1.08#	93.51 ± 4.35#	6.09 ± 1.16*#	1.58 ± 0.05*

* Sig (≤ 0.05) versus the control Gp; # Versus PPA-Gp.

with the control group. The PPA+EPO-Gp revealed a significant decrease in the mean values of serotonin levels compared to the control group, with no significant difference between them in the other parameters. In addition, PPA+EPO-Gp displayed a significant decrease in the mean values of MDA and a significant increase in the mean values of GSH-Px and GABA compared to PPA-Gp (Table 2).

Estimating the gene expression levels of EPO receptor (EPO R) in all studied groups

The cerebellar homogenate revealed a significant increase of EPO R that was estimated by qRT-PCR in PPA-Gp and PPA+EPO-Gp groups compared to the control group. The data revealed no significant difference regarding the expression levels of EPO R between PPA-Gp and PPA+EPO-Gp (Table 2).

EPO mitigated the cerebellar injury in PPA-induced autistic rats

The cerebellar cortex of the control rats exhibited three consecutive layers: the outer molecular, middle Purkinje, and inner granular layers. Sections from PPA-Gp showed obvious degeneration of PCs that were widely spaced by lost cells. Besides, the separation between granule cells in the granular layer was detected. The PPA+EPO-Gp demonstrated a normal histological architecture of the cerebellar cortex with a significant increase in the PCs count, demonstrating vesicular central nuclei and prominent nucleoli. (Fig. 1C–D)

EPO protected the PC neurofibril connectivity in PPA-induced autistic rats

Sections from the control rats showed PCs with regularly arranged nerve fibers in the molecular layer. In contrast, PPA-Gp exhibited many irregular dark brown nerve fibers in the molecular layer, which showed a significant increase in the optical density of Ag-positive reactions compared with the control and PPA+EPO-Gp groups. However, PPA+EPO-Gp showed regular nerve fibers in the molecular layer (Fig. 1E–H).

EPO protected against astrogliosis

Sections from PPA-Gp demonstrated enhanced astroglial activity in all cerebellar layers. Sections from PPA+EPO-Gp revealed decreased astroglial activity compared with that of PPA-Gp (Fig. 2A–D).

EPO protected against PCs degeneration

The control group showed strong cytoplasmic calbindin immunostaining in PCs and nerve fibers in the molecular layer. The PPA-Gp exhibited significantly reduced cytoplasmic calbindin immunostaining in distorted PCs and nerve fibers in the molecular layer. Meanwhile, PPA+EPO-Gp revealed strong positive cytoplasmic immunostaining in most PCs and nerve fibers in the molecular layer, which was comparable to that of the control (Fig. 3A–D).

Ultrastructural changes of Purkinje cells

The control group showed PCs with central euchromatic nuclei, well-defined, regular nuclear membranes, and prominent nucleoli. Their cytoplasm contained mitochondria, short cisternae of the rough endoplasmic reticulum (rER), polysomes, and a well-developed Golgi apparatus (Fig. 4A). Meanwhile, sections of the PPA-Gp revealed most PCs with irregular nuclei, chromatin clumps, and irregular nuclear membranes. Dilated cisternae in the rER, abnormally swollen mitochondria, and lysosomes were observed. Wide spaces surrounding PCs were also observed (Fig. 4B). In contrast to PPA+EPO-Gp, most PCs had central euchromatic nuclei with well-defined regular nuclear membranes and prominent nucleoli. The cytoplasm contained mitochondria, cisternae of the rER, polysomes, and a well-developed Golgi apparatus (Fig. 4C).

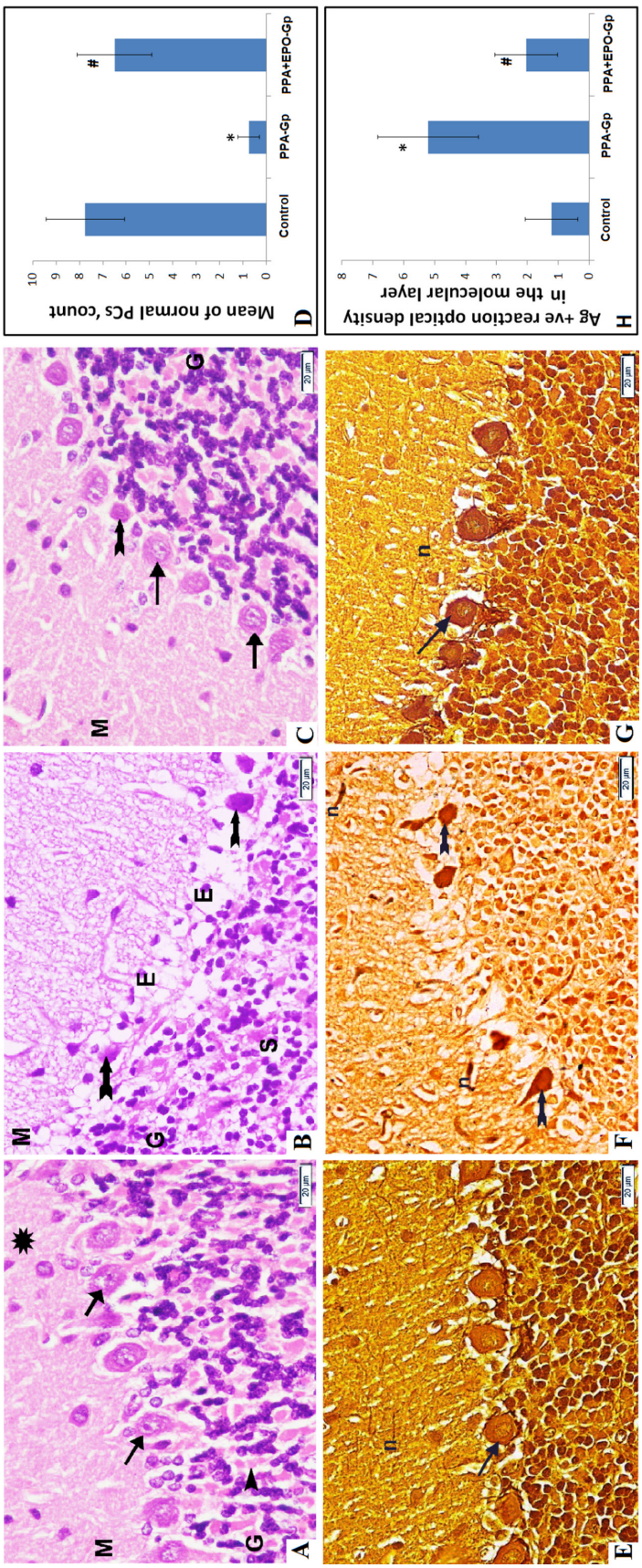

Fig. 1. Photomicrographs of H&E and Bielschowski's Ag-stained sections in the cerebellar cortex. (**A**) The control shows the molecular layer (M) containing a few widely separated basket cells (b) and acidophilic nerve fibers (asterisk). The Middle Purkinje cell layer contains one row of large Purkinje cells (arrow) with basophilic cytoplasm, central vesicular nuclei, and prominent nucleoli. The granular layer (G) contains numerous tightly packed small granule cells with dark rounded nuclei and acidophilic cerebellar islands, Mossy rosettes, (arrowhead) in-between. (**B**) PPA-Gp shows widely separated distorted deeply-stained Purkinje cells with pyknotic nuclei (bifid arrow), empty spaces (E), and separation (S) between granule cells in the granular layer. (**C**) PPA+EPO-Gp shows apparently normal histological architecture of the cerebellar cortex; molecular layer (M), granular layer (G), and Purkinje cells (arrow) with a distorted deeply stained Purkinje cell illustrating pyknotic nucleus (bifid arrow). (**D**) Quantification of the mean of Purkinje cells 'count. (**E**) The control shows Purkinje cells (arrow) with homogenous cytoplasm and fine regularly arranged nerve fibers (n) in the molecular layer. (**F**) PPA-Gp shows some widely separated distorted Purkinje cells (bifid arrow) and many irregular dark brown tangled nerve fibers (n) in the molecular layer. (**G**) PPA+EPO-Gp shows many Purkinje cells with homogenous brown-stained cytoplasm (arrow). The molecular layer shows regularly arranged nerve fibers (n). (**H**) Quantification of optical density of Ag + ve reaction in the molecular layer. (n = 8) (Magnification 400×) (* Significant (≤ 0.05) versus the control Gp; # Significant versus PPA-Gp).

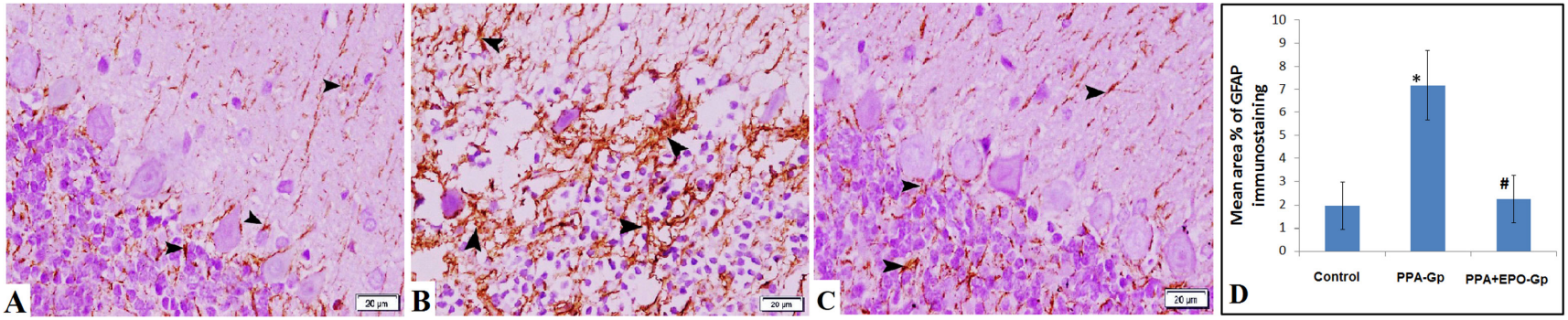

Fig. 2. Photomicrographs of GFAP immunostained sections in the cerebellar cortex. (**A**) The control exhibits few GFAP-positive astrocytes (arrowhead) with few thin processes in the granular layer, around Purkinje cells, and in molecular layer. (**B**) PPA-Gp shows numerous GFAP-positive astrocytes (arrowhead) with multiple thick interdigitating processes in the granular layer, around degenerated Purkinje cells, and in molecular layer. (**C**) PPA+EPO-Gp reveals few GFAP-positive astrocytes (arrowhead) with few thin processes in the granular layer, around Purkinje cells, and in the molecular layer. (**D**) Quantification of the mean area % of GFAP immunostaining. (* Significant (≤ 0.05) versus the control Gp; # Significant versus PPA-Gp). (n = 8) (Magnification 400×)

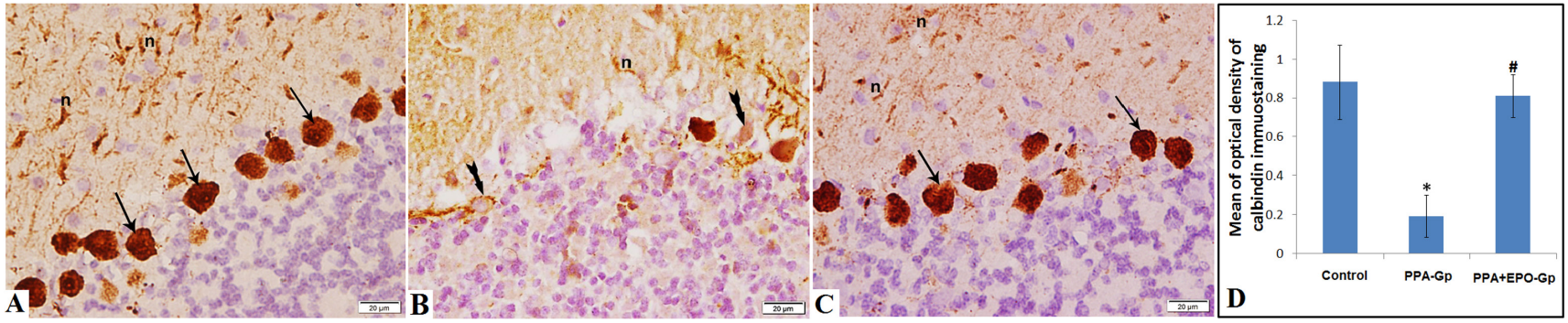

Fig. 3. Photomicrographs of calbindin D28K-immunostained sections in the cerebellar cortex. (**A**) The control exhibits strong positive cytoplasmic immunostaining in Purkinje cells (arrow) and nerve fibers (n) in the molecular layer. (**B**) PPA-Gp shows weak positive cytoplasmic immunostaining in the distorted Purkinje cells (bifid arrow) with few immunostained nerve fibers (n) in the molecular layer. (**C**) PPA+EPO-Gp reveals strong positive cytoplasmic immunostaining in numerous Purkinje cells (arrow) and nerve fibers (n) in the molecular layer. (**D**) Quantification of the mean optical density of calbindin immunostaining. * Significant (≤ 0.05) versus the control Gp; # Significant versus PPA-Gp. (n = 8) (Magnification 400×).

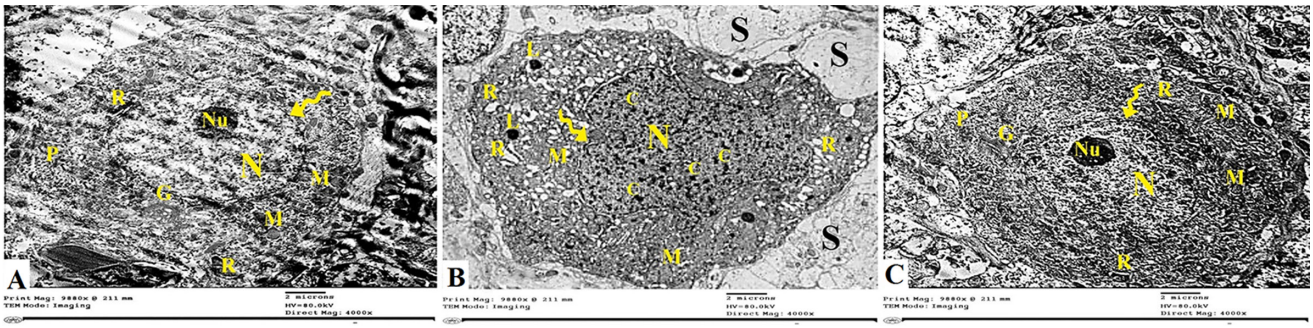

Fig. 4. Photomicrographs of ultra-thin sections in the Purkinje cells. (**A**) Purkinje cell in the control group shows a central euchromatic nucleus (N) with a well-defined regular nuclear envelope (zigzag arrow) and prominent nucleolus (Nu). The cytoplasm exhibits mitochondria (M), short cisternae of rER (R), polysomes (P), and well-developed Golgi apparatus (G). (**B**) Purkinje cell in PPA -Gp reveals an irregular nucleus (N) with chromatin clumps (C) and an irregular nuclear envelope (zigzag arrow). The cytoplasm exhibits dilated cisternae of rER (R), abnormally swollen mitochondria (M), and lysosomes (L). Wide spaces (S) surrounding the Purkinje cell are also seen. (**C**) Purkinje cell in PPA+EPO-Gp shows a central euchromatic nucleus (N) with a well-defined nuclear envelope (zigzag arrow) and prominent nucleolus (Nu). The cytoplasm shows mitochondria (M), short cisternae of rER (R), polysomes (P), and well-developed Golgi apparatus (G). (n = 8) (Magnification 4000×)

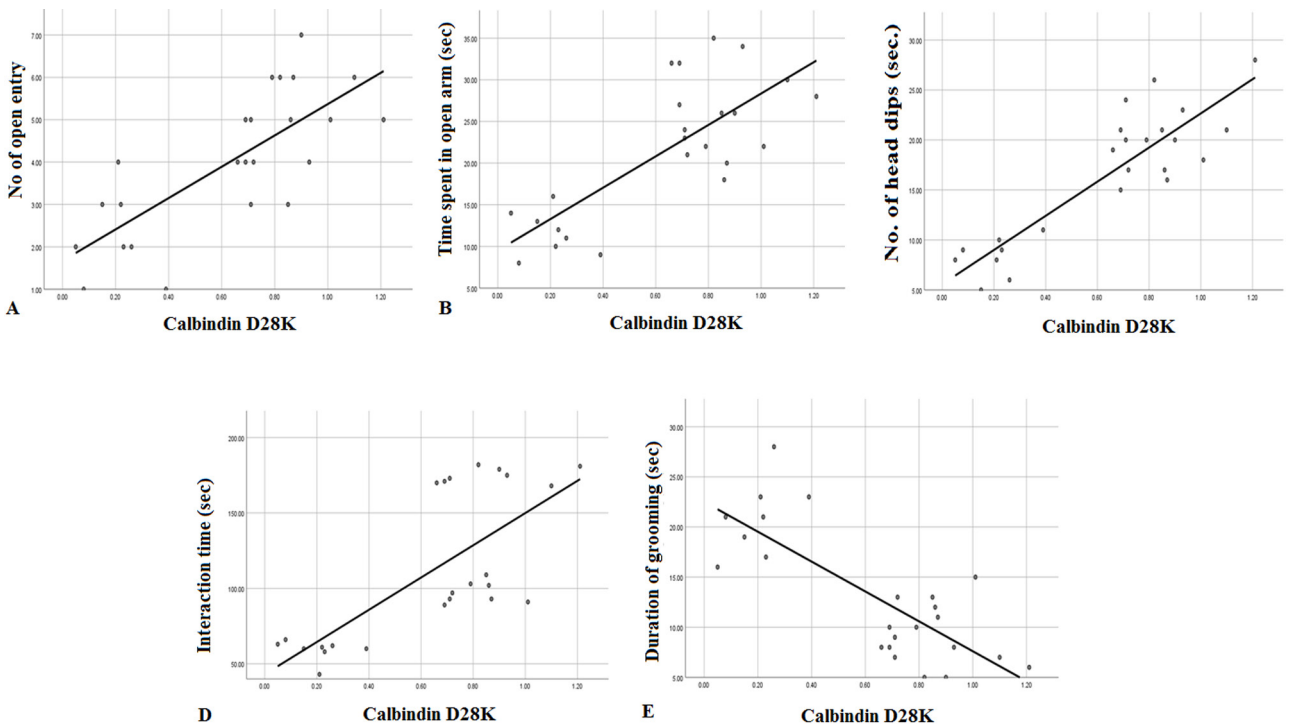

Fig. 5. Correlation between calbindin D28K immune-expression in the cerebellum and cognitive functions. Calbindin D28K immune expression displays a positive correlation with (**A**) the No. of open arm entry, (**B**) the time spent in open arm (Sec.), (**C**) the No. of head dipping from the other side, and (**D**) the duration of social interaction. (**E**) Represents a negative correlation between calbindin D28K and the duration of grooming. (n = 8)

Correlation results

The data demonstrated a strong association between calbindin% and the number of open arm entries ($r = 0.757$, $p < 0.001$), the amount of time spent in the open arm (Sec.) ($r = 0.771$, $p < 0.001$), the number of head dips ($r = 0.884$, $p < 0.001$), and the duration of social interaction (Sec.) ($r = 0.736$, $p < 0.001$). In addition, there was a negative correlation between calbindin% and grooming duration of grooming (Sec.) ($r = -0.779$, $p < 0.001$) (Fig. 5).

IV. Discussion

Autism spectrum disorder (ASD) is a neurodevelopmental disorder characterized by social-affective impairments and deficits in verbal and non-verbal communication. This study evaluated the possible neuroprotective effects of EPO in a PPA-induced autism model in young male rats using histological, immunohistochemical, electron microscopic, and biochemical analyses.

The cerebellum was selected for the study of autism

because of its pivotal role in the pathological changes in autism [5]. Recent research supported that the integrity of the cerebro-cerebellar loop is substantial cortical development and that its dysfunction can mediate deficits in motor control and provoke repetitive and stereotyped behaviors in ASD [10]. Previous brain studies have indicated the role for the cerebellum in the regulation of emotions and anxiety. A single session of repeated high-frequency transcranial magnetic stimulation (rTMS) to the medial cerebellum of healthy volunteers provoked a positive mood. Low frequency rTMS of the vermis has induced a negative mood [30, 31].

In the current study, we evaluated the behavioral response in rats exposed to PPA that was successfully able to induce autistic-like features, including significant anxiety and decreased social behaviors, compared to the control group. The high frequency of open-arm activity and head dipping is an indicator of exploration, less anxiety, and an attitude toward risk assessment. In addition, less fearful behavior can be confirmed by a decreased grooming duration [32]. In previous studies, PPA administration in rats exhibited changes in the synthesis and release of neurotransmitters, elevated levels of microglia and neurotoxic cytokines, including interleukin (IL)-6, tumor necrosis factor (TNF)-α, and interferon-γ, and abnormal behaviors, such as repetitive and deteriorated social interactions [12, 26].

Histological examination of the cerebellum in PPA-Gp showed obvious PC dysmorphology and a reduced count. Besides, a significant reduction in the levels of GSH-Px, GABA, and serotonin and a significant elevation in the MDA level were estimated in the brain tissue, indicating the extent of cellular oxidative injury, The accumulated neurofibrils caused global degenerative changes in neurons and their axons, resulting in disrupted myelination [3]. Previous studies have revealed a correlation between the induction of oxidative stress and the depletion of antioxidant enzymes, including GSH reductase, glutathione peroxidase, and superoxide dismutase, after PPA administration [12, 25]. Lobzhanidze *et al*., 2019 [22], documented that elevated oxidative stress caused an intense disturbance in the intercellular biochemical events and damage to the proteins, DNA, and lipid components inside the cell, resulting in degenerative changes in PCs. In addition, PPA declined the antioxidant defense system by decreasing GSH levels and increasing TNF-α and IL-6 levels, thereby increasing the cell liability for lipid peroxidation in different brain regions. Moreover, low levels of IL-10 promoted neuroinflammation. Neuroinflammation and oxidative damage have significant roles in neurodegeneration and neurodevelopmental changes [25].

In the present study, the cerebellum of PPA-treated rats showed marked astrogliosis, associated with a significant decrease in the optical density of calbindin, indicating PC degeneration. GABAergic signaling performed a critical role in brain development; thus, ASD pathogenesis is related to its disturbance. Classification of GABAergic neurons depends on the expression of Ca^{2+}-binding proteins such as calbindin D-28k, parvalbumin, and calretinin [7]. Previous studies have demonstrated that calbindin D-28k, which is expressed in PCs, is an essential determinant of normal motor coordination and sensory integration. The absence of calbindin from this neuron results in a novel mouse phenotype with distinct deficits in the precision of motor coordination and the processing of coordination-relevant visual information [5]. Whitney and colleagues (2008) [40] reported that calbindin-D28k is a more reliable marker that shows decreased PC numbers. The authors observed a decreased number of PCs in all cerebellar parts in the autism-like group compared with the control group. Our results showed that calbindin immunostaining was positively correlated with the number of open arm entries, duration in the open arm of the elevated plus maze, and duration of social interactions, whereas it was negatively correlated with grooming duration. This indicated a correlation with the severity of the autistic-like features.

In the present study, substantial protection was detected in PPA+EPO-Gp compared to that in PPA-Gp. EPO administration resulted in significantly improved behavioral assessment scoring and GABA levels as compared to PPA-Gp, with a comparable level to those of the control rats in the levels of GSH-Px and MDA. Golshani *et al*., 2019 [16], found that EPO improved the biochemical impairments that accompanied the neurodegeneration resulting from bile duct ligation. In a lipopolysaccharide-induced rat model of ASD, EPO decreased neuroinflammation, as indicated by reduced brain TNF-α levels, and improved social deficits as well [33]. In a randomized phase II trial that was conducted to study preterm infants' neuroprotection by EPO, the latter was able to decrease serum pro-inflammatory markers and improve brain injury biomarkers [18]. Additionally, EPO restored social deficits and increased interaction time in a rat model of prenatal transient hypoxia-ischemia-mediated brain injury [28].

The expression levels of EPO R were statistically evaluated and their mean values were significantly increased in the whole cerebellar tissue of PPA groups compared to the control group. In this context, Digicaylioglu and colleagues [8] identified the localization of EPO R in various regions of mouse and primate brains. Meanwhile, the activation of EPO R was suggested to exert a neuroprotective role. It was found that exposure to hypoxia can induce EPO R expression in neurons aiming for protection [38]. In in-vitro cultured cerebellar granule cells that were extracted from Wistar rats, the inhibition of Ca^{2+}-mediated glutamate release was mediated by both erythropoietin and the EPO R agonist, thus indicating the role of EPO-EPO R activation in preventing neuronal cell death [19].

The H&E examination of the PPA+EPO-Gp cerebellar cortex demonstrated an apparently normal histological architecture with a few distorted PCs. These findings were

supported by silver staining, which showed few distorted, faintly stained PCs among apparently normal cells with regular nerve fibers in the molecular layer, in addition to the preserved ultrastructural features of PCs, the significant increase in the mean number of apparently normal PCs, calbindin expression in PCs, and a significant decrease in astrogliosis compared to PPA-Gp. Rivera-Cervantes *et al*., 2019 [27] reported that treatment with EPO was associated with an increase in the number of normal cells with no observed cellular abnormalities in the brain, and no statistically significant differences were found regarding the control group. In a rat model of bile duct ligation-induced neuroinflammation, gliosis and neurodegeneration were significantly decreased by EPO administration [16]. Consequently, the antioxidant properties of EPO might be a probable mechanism of action, as EPO decreases the levels of reactive oxygen species and modulates inflammatory cytokines and mitochondrial dysfunction in rats [18]. EPO can execute multiple protective pathways, including the attenuation of inflammatory responses, inhibition of apoptosis, restoration of vascular autoregulation, restoration of cellular function, and promotion of angiogenesis and neurogenesis, which are crucial for the repair of normal and injured neurodevelopment [20].

In conclusion, this study demonstrated that EPO provided significant protection against PPA-induced autistic features in rats with structural preservation of PCs, alleviated gliosis in the cerebellar cortex, increased intercellular antioxidant levels, and suppressed neuroinflammation, suggesting its use as a promising neuroprotective approach in similar cases in the future.

Future studies are recommended to explore the exact site of EPO receptors localization in cerebellar layers and to identify the site of highest expression.

V. Limitation of the Study

The authors did not investigate what kinds of cells express EPO-R in the cerebellum in this study. Other brain regions, such as the hippocampus may also contribute to the behavioral improvement by EPO in this study, because PPA-induced neurodegeneration and EPO-mediated neuroprotection was observed not only in the cerebellum, but also in the hippocampus (supplementary material).

VI. Conflicts of Interest

The authors declare that there are no competing interests.

VII. References

1. Alfawaz, H. A., Bhat, R. S., Al-Ayadhi, L. and El-Ansary, A. K. (2014) Protective and restorative potency of Vitamin D on persistent biochemical autistic features induced in propionic acid-intoxicated rat pups. *BMC Complement. Altern. Med.* 14; 416.
2. Ali, E. H. A., Hassan, M. K., Abbas, O. A., Elmalahy, H. E. and Abu Almaaty, A. H. (2020) Urtica dioica improves brain dysfunctions in propionic acid autistic-like rat model through brain monoamines and mitochondrial energy. *African J. Biol. Sci.* 16; 207–231.
3. Arafat, E. A. and Shabaan, D. A. (2019) The possible neuroprotective role of grape seed extract on the histopathological changes of the cerebellar cortex of rats prenatally exposed to Valproic Acid: an animal model of autism. *Acta Histochem.* 121; 841–851.
4. Bancroft, J. D. and Layton, C. (2013) The hematoxylin and eosin. In "Theory & Practice of histological techniques (7th ed.)", ed. by S. K. Suvarna, C. Layton and J. D. Bancroft, Churchill Livingstone of El Sevier, Philadelphia, pp. 173–214.
5. Barski, J. J., Hartmann, J., Rose, C. R., Hoebeek, F., Mörl, K., Noll-Hussong, M., *et al.* (2003) Calbindin in cerebellar Purkinje cells is a critical determinant of the precision of motor coordination. *J. Neurosci.* 23; 3469–3477.
6. Choi, J., Lee, S., Won, J., Jin, Y., Hong, Y., Hur, T. Y., *et al.* (2018) Pathophysiological and neurobehavioral characteristics of a propionic acid-mediated autism-like rat model. *PLoS One* 13; e0192925.
7. Coghlan, S., Horder, J., Inkster, B., Mendez, M. A., Murphy, D. G. and Nutt, D. J. (2012) GABA system dysfunction in autism and related disorders: from synapse to symptoms. *Neurosci. Biobehav. Rev.* 36; 2044–2055.
8. Digicaylioglu, M., Bichet, S., Marti, H. H., Wenger, R. H., Rivas, L. A., Bauer, C., *et al.* (1995) Localization of specific erythropoietin binding sites in defined areas of the mouse brain. *Proc. Natl. Acad. Sci. U S A* 92; 3717–3720.
9. Ding, J., Wang, J., Li, Q. Y., Yu, J. Z., Ma, C. G., Wang, X., *et al.* (2017) Neuroprotection and CD131/GDNF/AKT pathway of carbamylated erythropoietin in hypoxic neurons. *Mol. Neurobiol.* 54; 5051–5060.
10. D'Mello, A. M. and Stoodley, C. J. (2015) Cerebro-cerebellar circuits in autism spectrum disorder. *Front. Neurosci.* 9; 408.
11. Eid, T. and Brines, M. (2002) Recombinant human erythropoietin for neuroprotection: what is the evidence? *Clin. Breast Cancer* 3; S109–S115.
12. El-Ansary, A. K., Ben Bacha, A. and Kotb, M. (2012) Etiology of autistic features: the persisting neurotoxic effects of propionic acid. *J. Neuroinflammation* 9; 74.
13. Estaphan, S., Curpăn, A. S., Khalifa, D., Rashed, L., Ciobica, A., Cantemir, A., *et al.* (2021) Combined low dose of ketamine and social isolation: a possible model of induced chronic schizophrenia-like symptoms in male albino rats. *Brain Sci.* 11; 917.
14. Flagstad, P., Mork, A., Glenthoj, B. Y., van Beek, J., Michael-Titus, A. T. and Didriksen, M. (2004) Disruption of neurogenesis on gestational day 17 in the rat causes behavioral changes relevant to positive and negative schizophrenia symptoms and alters amphetamine-induced dopamine release in nucleus accumbens. *Neuropsychopharmacology* 29; 2052–2064.
15. Gage, G. J., Kipke, D. R. and Shain, W. (2012) Whole animal perfusion fixation for rodents. *JoVE.* (65); e3564.
16. Golshani, M., Basiri, M., Shabani, M., Aghaei, I. and Asadi-Shekaari, M. (2019) Effects of erythropoietin on bile duct ligation-induced neuroinflammation in male rats. *AIMS Neurosci.* 6; 43–53.
17. Hashem, S., Nisar, S., Bhat, A. A., Yadav, S. K., Azeem, M. W., Bagga, P., *et al.* (2020) Genetics of structural and functional brain changes in autism spectrum disorder. *Transl. Psychiatry* 10; 229.
18. Juul, S. E., Mayock, D. E., Comstock, B. A. and Heagerty, P. J.

(2015) Neuroprotective potential of erythropoietin in neonates; design of a randomized trial. *Matern. Health. Neonatol. Perinatol.* 1; 27.
19. Kawakami, M., Sekiguchi, M., Sato, K., Kozaki, S. and Takahashi, M. (2001) Erythropoietin receptor-mediated inhibition of exocytotic glutamate release confers neuroprotection during chemical ischemia. *J. Biol. Chem.* 276; 39469–39475.
20. Li, Q., Han, Y., Du, J., Jin, H., Zhang, J., Niu, M., *et al.* (2018) Recombinant human erythropoietin protects against hippocampal damage in developing rats with seizures by modulating autophagy via the S6 protein in a time-dependent manner. *Neurochem. Res.* 43; 465–476.
21. Liu, H., Zhang, M. and Han, X. (2020) Therapeutic effect of erythropoietin on brain injury in premature mice with intrauterine infection. *Saudi. J. Biol. Sci.* 27; 2129–2133.
22. Lobzhanidze, G., Lordkipanidze, T., Zhvania, M., Japaridze, N., MacFabe, D. F., Pochkidze, N., *et al.* (2019) Effect of propionic acid on the morphology of the amygdala in adolescent male rats and their behavior. *Micron* 125; 102732.
23. MacFabe, D. F., Cain, N. E., Boon, F., Ossenkopp, K. P. and Cain, D. P. (2011) Effects of the enteric bacterial metabolic product propionic acid on object-directed behavior, social behavior, cognition, and neuroinflammation adolescent rats: Relevance to autism spectrum disorder. *Behav. Brain Res.* 217; 47–54.
24. Marti, H. H. (2004) Erythropoietin and the hypoxic brain. *J. Exp. Biol.* 207; 3233–3242.
25. Mirzaa, R. and Sharma, B. (2019) A selective peroxisome proliferator-activated receptor-γ agonist benefited propionic acid induced autism-like behavioral phenotypes in rats by attenuation of neuroinflammation and oxidative stress. *Chem. Biol. Interact.* 311; 108758.
26. Othman, M. A. M., Rajab, E., AlMubarak, A., AlNaisar, M., Bahzad, N. and Kamal, A. (2018) Erythropoietin protects against cognitive impairment and hippocampal neurodegeneration in diabetic mice. *Behav. Sci. (Basel).* 9; 4.
27. Rivera-Cervantes, M. C., Jarero-Basulto, J. J., Murguía-Castillo, J., Marín-Lopez, A. G., Gasca-Martínez, Y., Cornelio-Martínez, S., *et al.* (2019) The recombinant human erythropoietin administered in neonatal rats after excitotoxic damage induces molecular changes in the hippocampus. *Front. Neurosci.* 13; 118.
28. Robinson, S., Corbett, C. J., Winer, J. L., Chan, L. A. S., Maxwell, J. R., Anstine, C. V., *et al.* (2018) Neonatal erythropoietin mitigates impaired gait, social interaction and diffusion tensor imaging abnormalities in a rat model of prenatal brain injury. *Exp. Neurol.* 302; 1–13.
29. Rodríguez Cruz, Y., Strehaiano, M., Rodríguez Obaya, T., García Rodríguez, J. C. and Maurice, T. (2017) An intranasal formulation of erythropoietin (Neuro-EPO) prevents memory deficits and amyloid toxicity in the APPSwe transgenic mouse model of Alzheimer's disease. *J. Alzheimers Dis.* 55; 231–248.
30. Schutter, D. J. L. G., van Honk, J., d'Alfonso, A. A. L., Peper, J. S. and Panksepp, J. (2003) High frequency repetitive transcranial magnetic over the medial cerebellum induces a shift in the prefrontal electroencephalography gamma spectrum: a pilot study in humans. *Neurosci. Lett.* 336; 73–76.
31. Schutter, D. J. L. G. and van Honk, J. (2009) The cerebellum in emotion regulation: a repetitive transcranial magnetic stimulation study. *Cerebellum* 8; 28–34.
32. Settipani, C. A., Puleo, C. M., Conner, B. T. and Kendall, P. C. (2012) Characteristics and anxiety symptom presentation associated with autism spectrum traits in youth with anxiety disorders. *J. Anxiety Disord.* 26; 459–467.
33. Solmaz, V., Erdoğan, M. A., Alnak, A., Meral, A. and Erbaş, O. (2020) Erythropoietin shows gender dependent positive effects on social deficits, learning/memory impairments, neuronal loss and neuroinflammation in the lipopolysaccharide induced rat model of autism. *Neuropeptides* 83; 102073.
34. Sözmen, S. Ç., Kurul, S. H., Yiş, U., Tuğyan, K., Baykara, B. and Yılmaz, O. (2012) Neuroprotective effects of recombinant human erythropoietin in the developing brain of rat after lithium-pilocarpine induced status epilepticus. *Brain Dev.* 34; 189–195.
35. Tiwari, A., Khera, R., Rahi, S., Mehan, S., Makeen, H. A., Khormi, Y. H., *et al.* (2021) Neuroprotective effect of α-mangostin in ameliorating propionic acid-induced experimental model of autism in Wistar rats. *Brain Sci.* 11; 288.
36. Tsai, P. T., Rudolph, S., Guo, C., Ellegood, J., Gibson, J. M., Schaeffer, S. M., *et al.* (2018) Sensitive periods for cerebellar-mediated autistic-like behaviors. *Cell Rep.* 25; 357–367.
37. Vittori, D. C., Chamorro, M. E., Hernández, Y. V., Maltaneri, R. E. and Nesse, A. B. (2021) Erythropoietin and derivatives: Potential beneficial effects on the brain. *J. Neurochem.* 58; 1032–1057.
38. Wakhloo, D., Scharkowski, F., Curto, Y., Javed Butt, U., Bansal, V., Steixner-Kumar, A. A., *et al.* (2020) Functional hypoxia drives neuroplasticity and neurogenesis via brain erythropoietin. *Nat. Commun.* 11; 1313.
39. Wang, C. C., Lin, H. C., Chan, Y. H., Gean, P. W., Yang, Y. K. and Chen, P. S. (2013) 5-HT1A-receptor agonist modified amygdala activity and amygdala-associated social behavior in a valproate-induced rat autism model. *Int. J. Neuropsychopharmacol.* 16; 2027–2039.
40. Whitney, E. R., Kemper, T. L., Bauman, M. L., Rosene, D. L. and Blatt, G. J. (2008) Cerebellar Purkinje cells are reduced in a subpopulation of autistic brains: a stereological experiment using calbindin-d28k. *Cerebellum* 7; 406–416.